A Rank-Based EWMA TBEA Control Chart

Fernanda Otilia Figueiredo[1], Philippe Castagliola[*2], and Jean-Claude Malela-Majika[3]

[1]Universidade do Porto, Faculdade de Economia, Porto, Portugal & CEAUL, Faculdade de Ciências, Universidade de Lisboa, Portugal
[2]Nantes Université & LS2N UMR CNRS 6004, Nantes, France
[3]Department of Statistics, Faculty of Natural and Agricultural Sciences, University of Pretoria, Hatfield, Pretoria, South Africa

January 15, 2025

Abstract

Recently, considerable attention has been paid to the development of Time Between Events and Amplitude (TBEA) control charts. Almost all existing TBEA charts are of a parametric type. Parametric TBEA charts have the disadvantage of being very sensitive to deviations from the distributional assumptions and to the estimation of the process nominal parameters. This emphasizes the importance of developing nonparametric (or distribution-free) TBEA control charts. In this paper, a new distribution-free EWMA TBEA control chart based on the rank statistic, denoted as rank-based EWMA TBEA chart, for simultaneously monitoring the time interval between successive occurrences of an event and its magnitude is proposed. This chart is an extension of the Sign EWMA TBEA chart and uses a statistic close to the Wilcoxon Mann-Whitney statistic. The run length properties of the new TBEA chart are obtained by Markov chain techniques, and some numerical comparisons with other competing charts reveal its promising performance. An illustrative example is also provided to demonstrate the application and the implementation of the proposed TBEA control chart using real-world data.

Keywords: Control charts, distribution-free, Markov chain, statistical process monitoring, time between events and amplitude.

1 Introduction

In the field of Statistical Process Monitoring (SPM), various tools can be used to monitor processes; but, control charts are the most important tools to identify

[*]philippe.castagliola@univ-nantes.fr (corresponding author)

the presence of possible assignable causes that arises in manufacturing processes or any other types of processes. Several types of univariate parametric TBE (Time Between Events) control charts have been extensively developed in the literature in the last decade. TBE charts do not allow to simultaneously monitor the magnitude of an event and the time interval between successive occurrences of an event. Most of the existing TBE charts have been developed to monitor high quality processes and they often assume an exponential distribution for the TBE variable; but other possible distributions have also been recently considered in the literature. For a brief overview of univariate TBE control charts, we only refer to very recent works, and the references within help to complete the information; see, for example, Xie et al. (2022a), Xie et al. (2022b), Hu et al. (2023), Ahmad et al. (2023) and Dogu and ul Amin (2023), among others. Concerning the case of multivariate TBE control charts, the literature is more scarce; see, for instance, the bivariate TBE charts proposed in Xie et al. (2011) for exponential data, and Anojahatlo and Sabri-Laghaie (2022) for Gumbel's bivariate exponential data. For a more complete overview on multivariate TBE control charts, readers are referred to Zwetsloot et al. (2021).

The disadvantage of distribution-based charts is that they are very sensitive to the departure from the distributional assumptions and to the estimation of the process nominal parameters. This is very often encountered in real-world applications. Most of these control charts are based on the Sign statistic (SN) or the Wilcoxon Signed Rank (WSR) statistic and its variants, such as the statistics recently used in the design of nonparametric control charts in Celano et al. (2016), Tang et al. (2019), Perdikis et al. (2021a) and Perdikis et al. (2021b). Regarding nonparametric TBE charts, Castagliola et al. (2019) proposed a Phase 2 EWMA chart for count data based on the sign statistic, denoted as CEWMA SN chart, with exact run length properties. They reported that for a wide range of location shifts, the CEWMA SN chart outperforms the traditional EWMA sign and CUSUM sign charts considered in Yang et al. (2011) and Yang and Cheng (2011), respectively. Pehlivan and Testik (2010) analyzed the impact of the distributional assumption on the performance of EWMA charts when the assumption of exponential data is incorrect, and Ozsan et al. (2010) when the nominal process parameters are estimated. Zhang et al. (2014) also analyzed the effect of parameter estimation on the performance of the CUSUM-type charts, and Kumar and Chakraborti (2016) investigated the effect of parameter estimation on the performances of the Shewhart, CUSUM and EWMA charts. In all these studies, it was concluded that the misspecification of the model and the parameter estimation have a significant impact on the performance of the charts; but, they can be designed to be very robust to departures from the assumed distribution and to the estimation method. To avoid the requirement of a large Phase 1 dataset in the estimation of unknown parameters, Ali (2020) proposed a Bayesian TBE control chart. Johannssen et al. (2022) proposed a discrete TBE chart for monitoring the fraction of nonconforming in finite horizon processes and can also be used for both low-volume and mass production processes with frequent changeovers. Rizzo et al. (2020) proposed alternative performance metrics for discrete and continuous TBE control charts that can be more efficient than the traditional ones in some specific processes. For an overview on this type of control chart see, for instance, Chakraborti et al. (2001), Chakraborti et al. (2014), Chakraborti and Graham (2019a) and Chakraborti

and Graham (2019b).

This paper focuses on a different class of charts called TBEA (Time Between Events and Amplitude) control charts. TBEA charts are used to *simultaneously* monitor the time interval between occurrences of an event E and its magnitude. An event can be potentially disastrous and catastrophic according to its frequency and magnitude, having therefore a negative impact on the environment and/or living beings. These type of events can occur in different fields such as in environment, hydrology, meteorology, seismology, engineering, insurance, finance and biostatistics, among many others. TBEA charts only had a high development in the recent years, and almost all charts that we can find in the literature are univariate parametric charts, for simultaneously monitoring the time T between two occurrences of an event E and its magnitude X. Wu et al. (2009a) proposed a combined chart, called the $T\&X$ chart, assuming an exponential distribution for T and a gamma distribution for X, that exhibits a good performance for several type of shifts. Many other authors proposed the use of a single statistic that combines information from the two variables, for simultaneously monitoring T and X. Wu et al. (2009b) proposed a TBEA chart based on the ratio X/T that outperforms the charts proposed by Wu et al. (2009a), mainly in detecting sparse occurrences and/or small shifts in the magnitudes of an event. Wu and Qu (2010) proposed the G chart under the assumptions of exponential data for T and normal data for X, which outperforms the competing Shewhart charts proposed by Wu et al. (2009a) and Wu et al. (2009b). Qu et al. (2013) proposed the GCUSUM chart based on the G statistic, which is a function of T and X. This chart was found to be more effective in detecting out-of-control situations of an event, and outperformed its competitors. Cheng and Mukherjee (2014) proposed the use of a Hotelling T^2 chart after applying a Box-Cox transformation to the observed data (i.e. T and X). Cheng et al. (2017) proposed a MEWMA chart based on a bivariate gamma distribution and taking into account the dependence between the variables X and T. Qu et al. (2018) proposed the UCUSUM chart, which was found to be more effective than the other previous charts in detecting the increase in X and/or decrease in T. Ali and Pievatolo (2018) and Ali (2021) proposed the use of first passage time (FPT) charts that perform better than the ratio charts. Sanusi et al. (2020) proposed a Max-EWMA control chart based on the maximum of the absolute values of two EWMA statistics, one for controlling the magnitude X and the other for the frequency T of an event. Rahali et al. (2019) and Rahali et al. (2021) used three different statistics to construct Shewhart-type TBEA charts in order to monitor independent data from several distributions and correlated data respectively.

As mentioned earlier, parametric TBEA charts are based on *predefined* distributional assumptions for the time T between events and for the amplitude X of the event, which is a disadvantage. Wu et al. (2021) proposed a distribution-free EWMA TBEA control chart based on the Sign statistic. The new TBEA control chart proposed in this paper is an extension of the chart in Wu et al. (2021) that uses a statistic close to the Wilcoxon Mann-Whitney statistic.

The rest of this paper is organized as follows. In Section 2, a new rank-based statistic that combines information from the TBE and its amplitude is intro-

duced, and its distribution is also derived. Section 3 is devoted to the introduction of a new rank-based EWMA TBEA chart and how its run length properties can be obtained. Section 4 provides results concerning the optimal run length performance of the rank-based EWMA TBEA chart. In addition, Section 4 compares the proposed chart to the sign-based EWMA TBEA chart introduced in Wu et al. (2021). A real-world example to illustrate the application of the new proposed EWMA TBEA chart is considered in Section 5. Finally, some general conclusions are drawn in Section 6.

2 A rank-based TBEA statistic

Let $D_0 = 0, D_1, D_2, \ldots$ be the dates of occurrence of a specific *negative* event E. Let $T_1 = D_1 - D_0, T_2 = D_2 - D_1, \ldots$ be the time intervals between two consecutive occurrences of the event E and let $X_1, X_2, \ldots$ be the corresponding magnitudes of this event occurring at times $D_1, D_2, \ldots$ and assumed to be independent of $T_1, T_2, \ldots$ (see Figure 1). It must be noted that $D_0 = 0$ is the date of a "virtual" event which has no amplitude associated with. Let $F_X(x)$ and $F_T(t)$ be the *unknown* c.d.f. (cumulative distribution function) of the continuous variables X_i and T_i, $i = 1, 2, \ldots$, respectively.

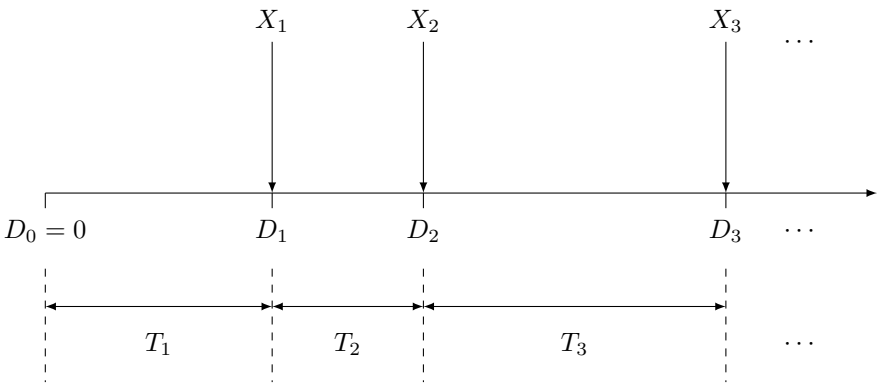

Figure 1: Times of occurrence D_i, time intervals T_i and amplitudes X_i of a negative event E

Let $\{X'_1, X'_2, \ldots, X'_m\}$ and $\{T'_1, T'_2, \ldots, T'_m\}$ be in-control (Phase 1) reference samples of size m associated with X and T, respectively. At every instant i of the process monitoring, consider the *combined* samples of size $m + 1$

$$\{X_i, X'_1, X'_2, \ldots, X'_m\} \text{ and } \{T_i, T'_1, T'_2, \ldots, T'_m\},$$

and rank the observations of each sample (i.e., assign rank 1 to the smallest value, rank 2 to the second smallest value, ..., rank $m + 1$ to the largest value). Because T_i and X_i are assumed to be continuous random variables, the occurrence of ties is not supposed to happen by definition, and this situation will not be considered in this paper. Nevertheless, in practice, some ties may occur. In such instances, each observation is given the mean of the ranks for which it

is tied. Note that even though there are ties the results will not be affected significantly.

In order to simultaneously monitor, in a distribution-free way, the time interval T_i between consecutive occurrences of the event E and its magnitude X_i, we suggest to denote RX_i and RT_i as the rank of X_i and T_i in the combined samples $\{X_i, X'_1, X'_2, \ldots, X'_m\}$ and $\{T_i, T'_1, T'_2, \ldots, T'_m\}$, respectively. Then, define the statistic R_i, $i = 1, 2, \ldots$ as

$$R_i = \mathrm{RX}_i - \mathrm{RT}_i. \tag{1}$$

The R_i statistic can be seen as the difference of two independent two-samples Wilcoxon statistics of parameters $(1, m)$. By definition (and as it is illustrated in Table 1), the R_i statistic is defined on $\{-m, -m+1, \ldots, -1, 0, 1, \ldots, m-1, m\}$. To justify the relevance of the R_i statistic for monitoring TBEA type processes, note that:

- R_i is small (negative value) when the process is in an *acceptable* situation, i.e. when T_i increases (RT_i gets larger) and, at the same time, X_i decreases (RX_i gets smaller).
- R_i is large (positive value) when the process is in an *unacceptable* situation, i.e. when T_i decreases (RT_i gets smaller) and, at the same time, X_i increases (RX_i gets larger).
- R_i is close to 0 when the process is in an *intermediate* situation, i.e. when both T_i and X_i increase or when both T_i and X_i decrease.

Table 1: Possible values of the statistic R_i as a function of RX_i and RT_i

		Acceptable ←			RT_i			→ Unacceptable
		$m+1$	m	$m-1$	$\cdots$	3	2	1
Unacceptable	$m+1$	0	1	2	$\cdots$	$m-2$	$m-1$	m
↑	m	-1	0	1	$\cdots$	$m-3$	$m-2$	$m-1$
	$m-1$	-2	-1	0	$\cdots$	$m-4$	$m-3$	$m-2$
RX_i	$\vdots$	$\vdots$	$\vdots$	$\vdots$	$\cdots$	$\vdots$	$\vdots$	$\vdots$
	3	$-m+2$	$-m+3$	$-m+4$	$\cdots$	0	1	2
↓	2	$-m+1$	$-m+2$	$-m+3$	$\cdots$	-1	0	1
Acceptable	1	$-m$	$-m+1$	$-m+2$	$\cdots$	-2	-1	0

Let $f_{\mathrm{RX}}(r)$ and $f_{\mathrm{RT}}(r)$, $r = 1, 2, \ldots, m+1$, be the p.m.f. (probability mass function) of the rank statistics RX_i and RT_i, respectively. If the process is *in-control*, i.e. the c.d.f. $F_X(x)$ of X_i ($F_T(t)$ of T_i) coincides with the c.d.f. of the corresponding reference sample $\{X'_1, X'_2, \ldots, X'_m\}$ ($\{T'_1, T'_2, \ldots, T'_m\}$), then the rank statistics RX_i and RT_i are simply i.i.d. (independent and identically distributed) random variables with a discrete uniform distribution over $\{1, 2, \ldots, m+1\}$ with p.m.f.

$$f_{\mathrm{RX}}(r) = f_{\mathrm{RT}}(r) = \frac{1}{m+1},\ r = 1, 2, \ldots, m+1. \tag{2}$$

When the process is *out-of-control* for the magnitude X_i, then the rank statistic RX_i is no longer a discrete uniform random variable with p.m.f. as in (2) and the corresponding p.m.f. $f_{\mathrm{RX}}(r)$ must have a

- negative asymmetric distribution with smaller values $f_{\mathrm{RX}}(r) < \frac{1}{m+1}$ when $r < \frac{m}{2}+1$ and larger values $f_{\mathrm{RX}}(r) > \frac{1}{m+1}$ when $r > \frac{m}{2}+1$, if X_i increases,
- positive asymmetric distribution with larger values $f_{\mathrm{RX}}(r) > \frac{1}{m+1}$ when $r < \frac{m}{2}+1$ and smaller values $f_{\mathrm{RX}}(r) < \frac{1}{m+1}$ when $r > \frac{m}{2}+1$, if X_i decreases.

For the out-of-control case, the same comments also apply to the rank statistic RT_i associated with the TBE T_i.

In order to obtain a realistic and easy-to-use model for the p.m.f. $f_{\mathrm{RX}}(r)$ of the rank statistic RX_i, including both the in- and out-of-control cases, we suggest to use an approach similar to the one proposed by Roy and Dasgupta (2001), which consists in defining the p.m.f. $f_{\mathrm{RX}}(r)$ and the c.d.f. $F_{\mathrm{RX}}(r)$, for $r = 1, 2, \ldots, m+1$, as

$$f_{\mathrm{RX}}(r) = F_\beta\left(\frac{r}{m+1}|a_{\mathrm{RX}}, b_{\mathrm{RX}}\right) - F_\beta\left(\frac{r-1}{m+1}|a_{\mathrm{RX}}, b_{\mathrm{RX}}\right), \tag{3}$$

$$F_{\mathrm{RX}}(r) = F_\beta\left(\frac{r}{m+1}|a_{\mathrm{RX}}, b_{\mathrm{RX}}\right), \tag{4}$$

respectively, where $F_\beta(\ldots|a_{\mathrm{RX}}, b_{\mathrm{RX}})$ is the c.d.f. of the beta distribution with parameters $a_{\mathrm{RX}} > 0$ and $b_{\mathrm{RX}} > 0$. This approach allows to obtain a bounded discrete distribution for $f_{\mathrm{RX}}(r)$ that mimics the shape of its continuous parent distribution (a beta distribution in our case) with the possibility to be either negative asymmetric or positive asymmetric (or even symmetric which coincides with the discrete uniform distribution). In order to keep this model simple, we have decided to define parameters a_{RX} and b_{RX} as a function of a single parameter $\pi_{\mathrm{RX}} \in (0, 1)$ such that

- $a_{\mathrm{RX}} = \frac{\pi_{\mathrm{RX}}}{1-\pi_{\mathrm{RX}}}$ and $b_{\mathrm{RX}} = 1$ if $\pi_{\mathrm{RX}} \in (0, 0.5]$,
- $a_{\mathrm{RX}} = 1$ and $b_{\mathrm{RX}} = \frac{1-\pi_{\mathrm{RX}}}{\pi_{\mathrm{RX}}}$ if $\pi_{\mathrm{RX}} \in [0.5, 1)$.

This definition ensures that π_{RX} coincides with the expectance of the beta distribution with parameters a_{RX} and b_{RX} and the special value $\pi_{\mathrm{RX}} = 0.5$ corresponds to $a_{\mathrm{RX}} = 1$ and $b_{\mathrm{RX}} = 1$, that is,the discrete uniform distribution over $\{1, 2, \ldots, m+1\}$ as in (2). By definition, π_{RX} can be seen as a *shift parameter* for the rank statistic RX_i. As an illustration, we represent in Figure 2 the p.m.f. given in (3) for $m = 10$ and $\pi_{\mathrm{RX}} \in \{0.3, 0.4, 0.5, 0.6, 0.7\}$. As it can be observed,

- if $\pi_{\mathrm{RX}} = 0.5$ then $f_{\mathrm{RX}}(r) = \frac{1}{11}$ (the dashed line) i.e. a discrete uniform distribution over $\{1, 2, \ldots, 11\}$. This corresponds with the in-control case for the amplitude X_i.
- if $\pi_{\mathrm{RX}} < 0.5$, we get a positive asymmetric distribution, i.e. small ranks RX_i with higher probabilities, and it means that the value of the amplitude X_i decreases.
- if $\pi_{\mathrm{RX}} > 0.5$, we get a negative asymmetric distribution, i.e. large ranks RX_i with higher probabilities, and it means that the value of the amplitude X_i increases. This case and the previous one correspond with the out-of-control case for the amplitude X_i.

Similar comments also apply to the rank statistic RT_i. The only thing that differs is that the terms a_{RX}, b_{RX} and π_{RX} must be replaced by a_{RT}, b_{RT} and π_{RT}. In the rest of this paper, we will refer to $f_{\mathrm{RX}}(r|\pi_{\mathrm{RX}})$ and $f_{\mathrm{RT}}(r|\pi_{\mathrm{RT}})$ to clearly emphasize the fact that these p.m.f. for RX_i and RT_i depend on the shift parameters π_{RX} and π_{RT}, respectively.

In the general case (in- or out-of-control situation), the p.m.f. $f_R(r|\pi_{\mathrm{RX}}, \pi_{\mathrm{RT}})$ of the statistic R_i can be obtained by convoluting the p.m.f. $f_{\mathrm{RX}}(r|\pi_{\mathrm{RX}})$ and $f_{\mathrm{RT}}(r|\pi_{\mathrm{RT}})$ of X_i and T_i

$$f_R(r|\pi_{\mathrm{RX}}, \pi_{\mathrm{RT}}) = \sum_{j=1}^{m+1} f_{\mathrm{RX}}(r+j|\pi_{\mathrm{RX}}) f_{\mathrm{RT}}(j|\pi_{\mathrm{RT}}), \tag{5}$$

and the expectation $\mathrm{E}(R_i)$ and variance $\mathrm{V}(R_i)$ of R_i are simply given by

$$\mathrm{E}(R_i) = \sum_{r=-m}^{m} r f_R(r|\pi_{\mathrm{RX}}, \pi_{\mathrm{RT}})$$

and

$$\mathrm{V}(R_i) = \sum_{r=-m}^{m} r^2 f_R(r|\pi_{\mathrm{RX}}, \pi_{\mathrm{RT}}) - \mathrm{E}(R_i)^2,$$

respectively. In the case where the process is assumed to be *in-control* for X_i and T_i (i.e. $\pi_{\mathrm{RX}} = \pi_{\mathrm{RT}} = 0.5$) then, using (2), it can be proven that

$$f_R(r|0.5, 0.5) = \frac{m+1-|r|}{(m+1)^2},\ r = -m, \ldots, m.$$

Since $f_R(r|0.5, 0.5) = f_R(-r|0.5, 0.5)$, the in-control p.m.f. of R_i is symmetric and its in-control expectation is

$$\mathrm{E}_0(R_i) = 0.$$

As demonstrated in the Appendix 1, the in-control variance $\mathrm{V}_0(R_i)$ of R_i is given by

$$\mathrm{V}_0(R_i) = \frac{m(m+2)}{6}.$$

3 A rank-based EWMA TBEA chart

To define and implement a rank-based EWMA TBEA type control chart we might monitor the R_i statistic using, for instance, the statistic $Z_i = \lambda R_i + (1-\lambda)Z_{i-1}$, where $\lambda \in (0, 1]$ is a smoothing parameter (usually a small value is recommended) and a starting value $Z_0 = 0$ is typically used. However, as already emphasized in Wu et al. (2021) and Wu et al. (2023), due to the discrete nature of the R_i statistic, the use of the standard Markov chain approach proposed by Brook and Evans (1972) (for CUSUM type control charts) for evaluating the RL (run length) performances leads to inaccurate and unstable values even if the number of Markov chain states is very large. In order to overcome this problem, using a similar approach as in Wu et al. (2021), we suggest to transform the

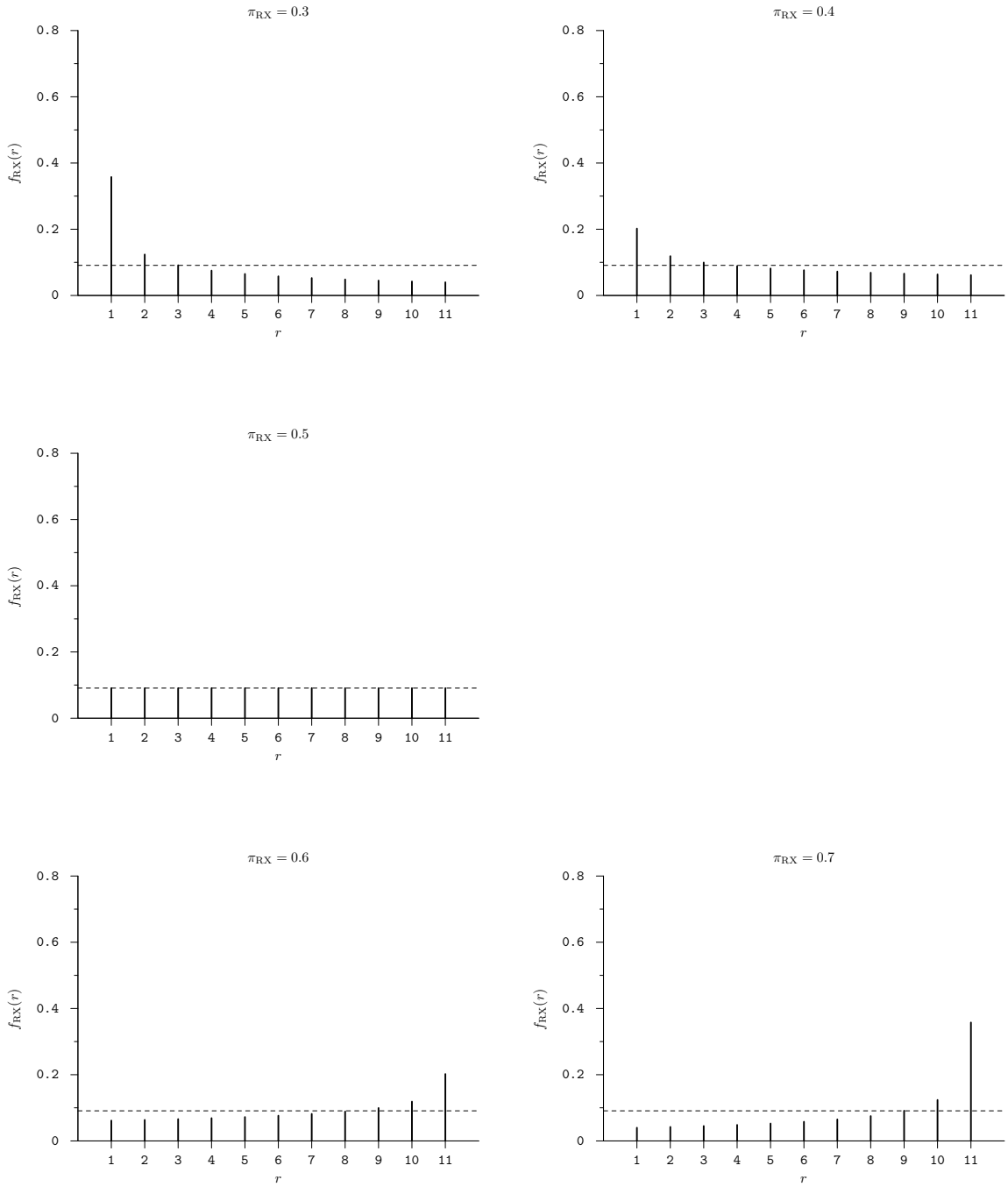

Figure 2: Examples of p.m.f. $f_{\mathrm{RX}}(r)$ for $m = 10$ and $\pi_{\mathrm{RX}} \in \{0.3, 0.4, 0.5, 0.6, 0.7\}$

discrete random variable R_i into a *new continuous* one, say R_i^*, and to consider the usual EWMA statistic with R_i replaced by R_i^*.

The method suggested by Wu et al. (2021) is named as the "continuousify" method and it consists in defining the new continuous statistic R_i^* as a mixture of $2m+1$ random normal variables $Y_{i,r} \sim \text{Nor}(r, \sigma)$, $r = -m, \ldots, m$, i.e. a mixture of random normal variables centered in the possible values of the random variable R_i, with a small standard deviation σ to avoid being overlapped, and with weights $w_r = f_R(r|\pi_{\text{RX}}, \pi_{\text{RT}})$.

The parameter $\sigma > 0$ has to be fixed and, as it has been shown in Wu et al. (2021) and Wu et al. (2023), its value does not significantly affect the run length distribution as long as it is neither too small nor too large. In this paper, we will use the value $\sigma = 0.125$ that has been suggested by Wu et al. (2021) and Wu et al. (2023) as a good trade-off.

Since the new statistic R_i^* is defined as a mixture of $2m+1$ random normal variables $Y_{i,r} \sim \text{Nor}(r, \sigma)$, $r = -m, \ldots, m$, its c.d.f. $F_{R^*}(r^*|\pi_{\text{RX}}, \pi_{\text{RT}})$ and p.m.f. $f_{R^*}(r^*|\pi_{\text{RX}}, \pi_{\text{RT}})$ are defined on $\mathbb{R}$ and they are equal to

$$F_{R^*}(r^*|\pi_{\text{RX}}, \pi_{\text{RT}}) = \sum_{r=-m}^{m} f_R(r|\pi_{\text{RX}}, \pi_{\text{RT}}) F_{\text{Nor}}\left(\frac{r^* - r}{\sigma}\right) \tag{6}$$

and

$$f_{R^*}(r^*|\pi_{\text{RX}}, \pi_{\text{RT}}) = \frac{1}{\sigma} \sum_{r=-m}^{m} f_R(r|\pi_{\text{RX}}, \pi_{\text{RT}}) f_{\text{Nor}}\left(\frac{r^* - r}{\sigma}\right), \tag{7}$$

respectively, where $F_{\text{Nor}}(\ldots)$ and $f_{\text{Nor}}(\ldots)$ denote the c.d.f. and p.d.f. of the standard normal distribution, respectively.

As the main objective of a TBEA type chart is to detect the occurrence of *negative* events rather than the occurence of positive ones. Thus in this paper, we will actually consider an *upper-sided* version of the EWMA statistic for R_i^* based on the statistic Z_i^* defined as follow

$$Z_i^* = \max(0, \lambda R_i^* + (1-\lambda) Z_{i-1}^*),\ i = 1, 2, \ldots \tag{8}$$

with a single asymptotic upper control limit, UCL, given by

$$\text{UCL} = \text{E}_0(R_i^*) + K\sqrt{\frac{\lambda}{2-\lambda}\text{V}_0(R_i^*)},$$

where initial value $Z_0^* = 0$, $\lambda \in (0, 1]$ and $K > 0$ are the control chart parameters, fixed and determined *a priori* to get a desirable in-control ARL (average run length), ARL_0. Using the same approach as in Wu et al. (2021) and Wu et al. (2023), it can be shown that $\text{E}_0(R_i^*) = \text{E}_0(R_i) = 0$ and $\text{V}_0(R_i^*) = \sigma^2 + \text{V}_0(R_i)$, which allows to obtain the following explicit formula for the upper control limit

$$\text{UCL} = K\sqrt{\frac{\lambda}{2-\lambda}\left(\sigma^2 + \frac{m(m+2)}{6}\right)}. \tag{9}$$

In order to assess the zero-state ARL and SDRL performance of the proposed upper-sided EWMA TBEA chart based on Z_i^*, we use the well-known Markov-chain approach, introduced by Brook and Evans (1972) that assumes that the behavior of the chart is well represented by a discrete-time Markov chain with $s+2$ states, $i = 0, 1, \ldots, s, s+1$, defined as follows:

- $i = 0$ is a transient state that corresponds to the "restart state" feature (due to the "max" in (8)) of the chart, and is represented by the value $H_0 = 0$;
- $i = 1, 2, \ldots, s$ are also transient states obtained by dividing the interval $[0, \text{UCL}]$ into s sub-intervals of width 2Δ, where $\Delta = \text{UCL}/2s$. The i-*th* state corresponds to the interval $]2(i-1)\Delta, 2i\Delta] =]H_i - \Delta, H_i + \Delta]$, and by definition, it is represented by its midpoint, equal to $H_i = (2i-1)\Delta$.
- $i = s+1$ is an absorbing state that corresponds to the out-of-control region $(\text{UCL}, +\infty)$ of the chart.

The transition probability matrix $\mathbf{P}$ of this discrete-time Markov chain is

$$\mathbf{P} = \begin{pmatrix} \mathbf{Q} & \mathbf{r} \\ \mathbf{0}^\intercal & 1 \end{pmatrix} = \begin{pmatrix} Q_{0,0} & Q_{0,1} & \cdots & Q_{0,s} & r_0 \\ Q_{1,0} & Q_{1,1} & \cdots & Q_{1,s} & r_1 \\ \cdots & \cdots & \cdots & \cdots & \cdots \\ Q_{s,0} & Q_{s,1} & \cdots & Q_{s,s} & r_s \\ 0 & 0 & \cdots & 0 & 1 \end{pmatrix},$$

where $\mathbf{Q}$ is the $(s+1, s+1)$ matrix of transient probabilities and the $(s+1, 1)$ vector $\mathbf{r}$ satisfies $\mathbf{r} = \mathbf{1} - \mathbf{Q}\mathbf{1}$, with $\mathbf{0} = (0, 0, \ldots, 0)^\intercal$ and $\mathbf{1} = (1, 1, \ldots, 1)^\intercal$. The generic element $Q_{i,j}$, $i = 0, 1, \ldots, s$, of the matrix $\mathbf{Q}$ is equal to:

- $Q_{i,0} = F_{R^*}\left(-\frac{(1-\lambda)H_i}{\lambda} | \pi_{\text{RX}}, \pi_{\text{RT}}\right)$, for $j = 0$,
- $Q_{i,j} = F_{R^*}\left(\frac{H_j + \Delta - (1-\lambda)H_i}{\lambda} | \pi_{\text{RX}}, \pi_{\text{RT}}\right) - F_{R^*}\left(\frac{H_j - \Delta - (1-\lambda)H_i}{\lambda} | \pi_{\text{RX}}, \pi_{\text{RT}}\right)$, for $j = 1, 2, \ldots, s$,

with $F_{R^*}(\ldots)$ defined as in (6). Let $\mathbf{q} = (q_0, q_1, \ldots, q_s)^\intercal$ be the $(s+1, 1)$ vector of initial probabilities associated with the $s+1$ transient states. In this paper we assume that $\mathbf{q} = (1, 0, \ldots, 0)^\intercal$, i.e. the initial state corresponds to the restart state $i = 0$. When the number s of subintervals considered in the discretization is sufficiently large, we obtain a good approximation for the transition probability matrix $\mathbf{P}$ of this discrete-time Markov chain that allows to accurately evaluate the zero-state ARL and SDRL of the chart using the following classical formulas,

$$\text{ARL} = \mathbf{q}^\intercal (\mathbf{I} - \mathbf{Q})^{-1} \mathbf{1}, \tag{10}$$

$$\text{SDRL} = \sqrt{2\mathbf{q}^\intercal (\mathbf{I} - \mathbf{Q})^{-2} \mathbf{Q}\mathbf{1} + \text{ARL}(1 - \text{ARL})}, \tag{11}$$

where $\mathbf{I}$ is the (s, s) identity matrix. The above formulas have been implemented using the Matlab-like software *SciLab* (`https://www.scilab.org/`) and the main functions are presented in Appendix 2.

4 Numerical analysis

The first goal of this section is to obtain optimal (λ^*, K^*) combinations for the proposed rank-based EWMA TBEA chart parameters (λ, K) that minimize the out-of-control $\text{ARL}(\lambda^*, K^*, \pi_{\text{RX}}, \pi_{\text{RT}})$ for $\pi_{\text{RX}} \neq 0.5$ and $\pi_{\text{RT}} \neq 0.5$ under the constraint $\text{ARL}(\lambda^*, K^*, 0.5, 0.5) = \text{ARL}_0$, where ARL_0 is a predefined value for the in-control ARL. The optimal values for (λ^*, K^*) are listed in Table 2 (first row) with the corresponding out-of-control values of (ARL, SDRL) (second row) for $\sigma = 0.125$ (the continuousify parameter), $m \in \{10, 20, 50\}$ (the Phase 1 sample size), $\pi_{\text{RT}} \in \{0.1, 0.2, \ldots, 0.4\}$ (as we are only interested in a decrease in T), $\pi_{\text{RX}} \in \{0.5, 0.6, \ldots, 0.9\}$ (as we are only interested in an increase in X) and assuming $\text{ARL}_0 = 370.4$. For instance, in Table 2, when $m = 20$, $\pi_{\text{RT}} = 0.4$ and $\pi_{\text{RX}} = 0.6$ the optimal chart parameters are $(\lambda^*, K^*) = (0.07, 2.5182)$ and the corresponding values for the out-of-control (ARL, SDRL) are ARL = 24.1 and SDRL = 15.6. From Table 2, we can draw the following conclusions:

- Regardless of the value of $m \in \{10, 20, 50\}$, when $\pi_{\text{RT}} = \pi_{\text{RX}} = 0.5$ we *exactly* obtain, as expected, $\text{ARL} = \text{ARL}_0 = 370.4$. In this case, it exists an infinite number of couples (λ^*, K^*) *exactly* satisfying the constraint $\text{ARL} = \text{ARL}_0 = 370.4$. These couples are denoted with "(–,–)" in Table 2.

- The out-of-control ARL and SDRL values monotonically decrease when the values of π_{RT} decrease and/or the values of π_{RX} increase. Due to the symmetry of RT_i and RX_i in the definition of the random variable R_i, the performance of the rank-based EWMA TBEA chart is identical for any combination of $(\pi_{\text{RT}} = \alpha_T, \pi_{\text{RX}} = \alpha_X)$ or $(\pi_{\text{RT}} = 1 - \alpha_X, \pi_{\text{RX}} = 1 - \alpha_T)$ where α_T and α_T are two values in $[0, 1]$. For this reason, in Table 2, only the lower side of each table is presented (the upper side can be obtained by symmetry). For example, if $m = 20$, the optimal parameters (λ^*, K^*) and corresponding out-of-control ARL and SDRL for $\pi_{\text{RT}} = 0.4$ and $\pi_{\text{RX}} = 0.7$ are the same as the ones for $\pi_{\text{RT}} = 0.3$ and $\pi_{\text{RX}} = 0.6$, i.e. $(\lambda^* = 0.14, K^* = 2.6576)$, ARL = 13.5 and SDRL = 8.5.

- The out-of-control ARL and SDRL values also monotonically decrease when the Phase 1 sample size m increases but at a rate that can be considered as negligible. For instance, when $\pi_{\text{RT}} = 0.4$ and $\pi_{\text{RX}} = 0.6$, we have $(\text{ARL}, \text{SDRL}) = (24.6, 15.9)$ when $m = 10$, $(\text{ARL}, \text{SDRL}) = (24.1, 15.6)$ when $m = 20$ and $(\text{ARL}, \text{SDRL}) = (23.9, 15.4)$ when $m = 50$. As a consequence, the Phase 1 sample size m seems to only have a marginal impact on the RL efficiency of the rank-based EWMA TBEA chart.

The second goal of this section is to compare the efficiency of the rank-based EWMA TBEA chart proposed in this paper with the sign-based EWMA TBEA chart proposed by Wu et al. (2021) (which has already been proven to be more efficient than the parametric Shewhart control charts proposed by Rahali et al. (2019)). In order to do that we must define equivalent shift parameters:

- in the current paper, the shift parameters are π_{RX} and π_{RT}. Their values reflect how the ranks RX_i and RT_i are distributed through Equation (3) based on the beta distribution.

- in Wu et al. (2021), the shift parameters are $p_T = \text{P}(T_i > \theta_{T_0}|\theta_T) = 1 - F_T(\theta_{T_0}|\theta_T)$ and $p_X = \text{P}(X_i > \theta_{X_0}|\theta_X) = 1 - F_X(\theta_{X_0}|\theta_X)$, where θ_{T_0},

Table 2: Optimal values for (λ^*, K^*) with the corresponding out-of-control values of $(\mathrm{ARL}, \mathrm{SDRL})$ for $\sigma = 0.125$, $m \in \{10, 20, 50\}$, $\pi_{\mathrm{RX}} \in \{0.5, 0.6, 0.7, 0.8, 0.9\}$ and $\pi_{\mathrm{RT}} \in \{0.1, 0.2, 0.3, 0.4, 0.5\}$

$m = 10$

	π_{RX}				
π_{RT}	0.5	0.6	0.7	0.8	0.9
0.5	(–,–) (370.4,–)				
0.4	(0.02,2.0874) (59.7,39.5)	(0.07,2.5180) (24.6,15.9)			
0.3	(0.06,2.4760) (25.6,15.8)	(0.13,2.6462) (13.9,8.6)	(0.22,2.6923) (8.9,5.4)		
0.2	(0.10,2.6007) (14.9,8.3)	(0.20,2.6890) (9.2,5.4)	(0.39,2.6453) (6.2,3.9)	(0.48,2.5955) (4.5,2.6)	
0.1	(0.15,2.6659) (10.1,5.1)	(0.30,2.6808) (6.7,3.8)	(0.42,2.6292) (4.7,2.6)	(0.59,2.5159) (3.5,1.8)	(0.80,2.3432) (2.8,1.2)

$m = 20$

	π_{RX}				
π_{RT}	0.5	0.6	0.7	0.8	0.9
0.5	(–,–) (370.4,–)				
0.4	(0.02,2.0876) (58.8,38.7)	(0.07,2.5182) (24.1,15.6)			
0.3	(0.06,2.4764) (24.8,15.2)	(0.14,2.6576) (13.5,8.5)	(0.28,2.6879) (8.6,5.6)		
0.2	(0.11,2.6195) (14.3,8.1)	(0.21,2.6921) (8.9,5.2)	(0.37,2.6568) (5.9,3.6)	(0.94,2.2983) (4.0,3.4)	
0.1	(0.16,2.6735) (9.5,4.9)	(0.32,2.6763) (6.4,3.6)	(0.48,2.5974) (4.4,2.5)	(0.95,2.2869) (2.8,2.1)	(0.95,2.2869) (1.9,1.2)

$m = 50$

	π_{RX}				
π_{RT}	0.5	0.6	0.7	0.8	0.9
0.5	(–,–) (370.4,–)				
0.4	(0.03,2.2478) (58.4,41.6)	(0.07,2.5185) (23.9,15.4)			
0.3	(0.06,2.4763) (24.5,14.9)	(0.14,2.6575) (13.3,8.3)	(0.29,2.6859) (8.4,5.5)		
0.2	(0.11,2.6193) (13.9,7.8)	(0.23,2.6940) (8.7,5.2)	(0.41,2.6384) (5.8,3.7)	(0.87,2.3260) (3.7,2.9)	
0.1	(0.17,2.6795) (9.2,4.7)	(0.34,2.6699) (6.1,3.6)	(0.87,2.3260) (4.0,3.1)	(0.88,2.3196) (2.6,1.8)	(0.95,2.2944) (1.8,1.2)

θ_{X_0} are the in-control median values (assumed to be known) for T_i, X_i, respectively, and θ_T, θ_X are the actual (out-of-control) median values.

Since the in-control median values θ_{T_0}, θ_{X_0} correspond to a rank $\mathrm{RX}_i = \mathrm{RT}_i = \frac{m}{2} + 1$, then we must have

$$p_T = \mathrm{P}\left(\mathrm{RT}_i > \frac{m}{2} + 1 | \pi_{\mathrm{RT}}\right) = 1 - F_{\mathrm{RT}}\left(\frac{m}{2} + 1 | \pi_{\mathrm{RT}}\right),$$
$$p_X = \mathrm{P}\left(\mathrm{RX}_i > \frac{m}{2} + 1 | \pi_{\mathrm{RX}}\right) = 1 - F_{\mathrm{RX}}\left(\frac{m}{2} + 1 | \pi_{\mathrm{RX}}\right),$$

and using (4) for both RX_i and RT_i simply gives

$$p_T = 1 - F_\beta\left(0.5 | a_{\mathrm{RT}}, b_{\mathrm{RT}}\right) \tag{12}$$

and

$$p_X = 1 - F_\beta\left(0.5 | a_{\mathrm{RX}}, b_{\mathrm{RX}}\right). \tag{13}$$

Since a_{RT} and b_{RT} depend on π_{RT}, and a_{RX} and b_{RX} depend on π_{RX}, we have equations that link p_T with π_{RT} and p_X with π_{RX}. More specifically, it is possible to obtain values of π_{RT} and π_{RX} for selected values of p_T and p_X by numerically solving Equations (12) and (13). The values of π_{RT} or π_{RX} are given in Table 3 for values of p_T or $p_X \in \{0.1, 0.2, \ldots, 0.9\}$. As it can be noticed in Table 3, the values of π_{RT} or π_{RX} are of course different from the ones of p_T or p_X but not significantly so different.

Table 3: Values of π_{RT} or π_{RX} for values of p_T or $p_X \in \{0.1, 0.2, \ldots, 0.9\}$.

p_T or p_X	π_{RT} or π_{RX}
0.1	0.132
0.2	0.244
0.3	0.340
0.4	0.424
0.5	0.500
0.6	0.576
0.7	0.660
0.8	0.756
0.9	0.868

Table 4 provides a comparison between the sign-based EWMA TBEA chart proposed by Wu et al. (2021) and the rank-based EWMA TBEA chart introduced in this paper. The table corresponding to the sign-based EWMA TBEA chart is a copy of the one already published by Wu et al. (2021). It has the same structure as the ones used in Table 2. The one for the rank-based EWMA TBEA chart has been obtained for $m = 10$ and for the same values of p_T and p_X (converted into π_{RT} and π_{RX} using Table 3). As it can be seen, the values of the out-of-control ARL and SDRL for the rank-based EWMA TBEA chart are all smaller than the ones for the sign-based EWMA TBEA chart (see values in bold in Table 4). For instance, if $p_T = 0.4$ and $p_X = 0.6$ (i.e. $\pi_{\mathrm{RT}} = 0.424$ and $\pi_{\mathrm{RX}} = 0.576$) we have $(\mathrm{ARL}, \mathrm{SDRL}) = (51.11, 32.63)$ for the sign-based EWMA

TBEA chart while they reduce to $(35.6, 24.2)$ for the rank-based EWMA TBEA chart. This proves the superiority of the rank-based EWMA TBEA chart over the sign-based EWMA TBEA chart.

5 Illustrative example

In this section, we consider the same illustrative example as the one used in Rahali et al. (2019) and Wu et al. (2021), which is based on real-world data concerning the time T_i (in days) between fires in forests of the french region "Provence - Alpes - Côte D'Azur" and their amplitudes X_i (burned surface in $ha = 10000m^2$, where only surfaces larger than $1ha$ have been included). This dataset reports a total of 92 fires that have been divided into two subsets:

- 47 fires (i.e., $m = 47$) collected from October 2016 to approximately mid-June 2017. This subset, corresponding to the "low season" for fires, is used here as a Phase 1 dataset.
- 45 fires (i.e., $n = 45$) collected from approximately mid-June 2017 to the end of September 2017. This subset, corresponding to the "high season" for fires, is used here as a Phase 2 dataset.

The dates D_i (from October 1st 2016, in days), the times between fires T_i as well as their amplitudes X_i have been recorded in Table 5. The values of T_i and X_i are also plotted in Figure 4 (top and middle) and, by observing these figures, it is evident that the Phase 2 values of T_i (X_i) are shorter (larger) than those observed during the Phase 1. In order to better understand the situation, some boxplots have been constructed for the Phase 1 and Phase 2 datasets (see Figure 3). We can easily see that the values of T_i in the high season are much smaller and with less dispersion than those in the low season. Moreover, in the high season, we have very large fires (see the outliers of variable X_i) which do not occur in the low season.

The method proposed in this paper assumes that the T_i and X_i are independant random variables. If we cannot test for independance we can, at least, check for *uncorrelation*. The value of the sample Spearman's rank correlation coefficient between the X_i and T_i is found to be $r_S = -0.136751$, and we get a p-value of 0.1937 when we test $H_0 : \rho_S = 0$ vs. $H_1 : \rho_S \neq 0$, where ρ_S denotes the Spearman's rank correlation coefficient. This leads us to conclude that, at a significance level of 0.05, the variables X_i and T_i are not correlated.

In order to compute the UCL of the proposed rank-based EWMA TBEA chart, the following values have been fixed: $\pi_T = 0.3$, $\pi_X = 0.7$, $\sigma = 0.125$ and $\mathrm{ARL}_0 = 370.4$. For these values, the optimal parameters are found to be equal to $\lambda^* = 0.29$ and $K^* = 2.6859$ and we easily obtain

$$\mathrm{UCL} = 2.6859 \times \sqrt{\frac{0.29}{2 - 0.29}\left(0.125^2 + \frac{47(47+2)}{6}\right)} = 21.67.$$

For the Phase 2 sample, Table 5 also records

- the ranks RX_i and RT_i as defined in Section 2.

Table 4: Comparison of the rank-based EWMA TBEA chart proposed in this paper with the sign-based EWMA TBEA chart proposed in Wu et al. (2021)

	Rank-based EWMA TBEA chart						Sign-based EWMA TBEA chart proposed in Wu et al. (2021)					
			p_X						p_X			
p_T	0.5	0.6	0.7	0.8	0.9		0.5	0.6	0.7	0.8	0.9	
0.5	(–,–) (370.4,–)						(–,–) (370.40,–)					
0.4	(0.02,2.0874) (**80.4**,**58.6**)	(0.05,2.4224) (**35.6**,**24.2**)					(0.010,1.774) (106.19,74.55)	(0.025,2.174) (51.11,32.63)				
0.3	(0.04,2.3502) (**34.0**,**21.2**)	(0.09,2.5788) (**19.7**,**12.5**)	(0.15,2.6659) (**12.5**,**7.7**)				(0.025,2.174) (51.88,32.87)	(0.045,2.387) (30.79,18.25)	(0.070,2.515) (20.68,11.53)			
0.2	(0.08,2.5517) (**18.4**,**10.6**)	(0.15,2.6659) (**12.2**,**7.3**)	(0.23,2.6929) (**8.5**,**5.0**)	(0.40,2.6404) (**5.9**,**3.7**)			(0.040,2.348) (31.53,17.72)	(0.065,2.496) (20.91,11.27)	(0.100,2.592) (14.99,7.80)	(0.140,2.638) (11.32,5.57)		
0.1	(0.13,2.6462) (**11.3**,**5.9**)	(0.21,2.6909) (**8.1**,**4.4**)	(0.39,2.6453) (**5.9**,**3.6**)	(0.49,2.5891) (**4.3**,**2.4**)	(0.62,2.4921) (**3.2**,**1.6**)		(0.060,2.474) (21.57,10.92)	(0.090,2.572) (15.30,7.50)	(0.135,2.634) (11.44,5.49)	(0.175,2.648) (8.88,3.89)	(0.225,2.639) (7.10,2.75)	

- the statistic $R_i = \mathrm{RX}_i - \mathrm{RT}_i$ as defined in (1).
- the "continuousified" statistics R_i^* obtained as explained in Section 3. As an example, at $D_i = 258$ we have $R_i = -8$ and the corresponding value R_i^* has been generated as a $\mathrm{Nor}(-8, \sigma)$ random number, $R_i^* = -7.948$ in our case.
- the EWMA statistic Z_i^* as defined in (8).

Based on Table 5 and on Figure 4 (bottom), the proposed rank-based EWMA TBEA chart detects several out-of-control situations during the period mid-June 2017 – end of September 2017, at dates $D_i = 289, 296, 297$ (see also the boldface values in Table 5), confirming that a decrease in the time between fires occurred with a concurrent increase in the amplitude of these fires. Similar conclusions have been obtained using the parametric approach in Rahali et al. (2019) and the nonparametric one in Wu et al. (2021).

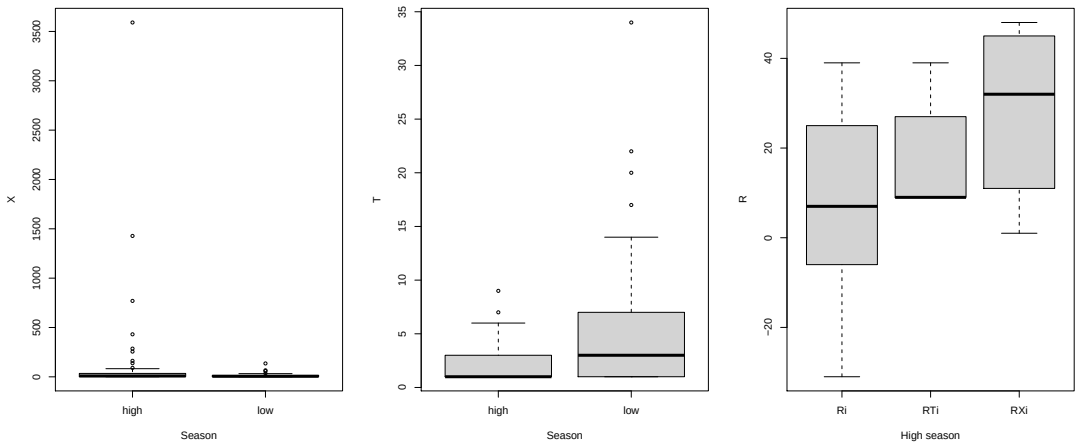

Figure 3: Boxplots for the data set by season, X_i (left) and T_i (middle), and for the values R_i (right) computed for the high season data.

6 Conclusions

The rank-based EWMA TBEA chart proposed in this paper is a distribution-free control chart and, therefore, it does not have the limitations of its parametric counterparts, where the choice of the distributions to model the variables T and X have to be made a priori, as well as the estimation of the corresponding parameters. Even without any particular assumption about the data distribution of X and T, and with only small Phase 1 reference samples, some numerical simulations have shown interesting run length performance of the chart. In particular, this chart has better out-of-control performance to simultaneously monitor the time between consecutive events and the amplitude of the events than the Sign-EWMA TBEA chart. The latter has a better performance as compared to the existing parametric Shewhart TBEA control charts that are

Table 5: Phase 1 and Phase 2 values of D_i, X_i, T_i and Phase 2 values of RX_i, RT_i, R_i, R_i^* and Z_i^* for the forest fires example.

Phase 1			Phase 2							
D_i	X_i	T_i	D_i	X_i	T_i	RX_i	RT_i	R_i	R_i^*	Z_i^*
9	3.68	9	258	1.00	1	1.0	9.0	-8.0	-7.948	0.000
26	1.99	17	260	3.70	2	18.0	20.0	-2.0	-2.021	0.000
60	6.00	34	262	3.17	2	14.0	20.0	-6.0	-5.999	0.000
67	1.19	7	265	18.40	3	38.0	27.0	11.0	10.811	3.135
70	135.80	3	268	1.00	3	1.0	27.0	-26.0	-25.948	0.000
72	14.37	2	269	2.22	1	11.0	9.0	2.0	2.026	0.587
86	8.10	14	271	19.09	2	39.0	20.0	19.0	18.941	5.910
88	32.31	2	272	2.00	1	11.0	9.0	2.0	2.012	4.780
94	3.07	6	274	34.28	2	44.5	20.0	24.5	24.309	10.443
95	10.03	1	276	3.00	2	13.0	20.0	-7.0	-7.275	5.305
96	7.93	1	277	6.63	1	29.0	9.0	20.0	19.718	9.485
97	1.50	1	278	4.47	1	21.0	9.0	12.0	11.953	10.201
103	23.30	6	285	8.24	7	31.0	36.5	-5.5	-5.469	5.656
106	3.73	3	286	769.45	1	48.0	9.0	39.0	39.027	15.334
109	4.73	3	287	4.37	1	20.0	9.0	11.0	10.955	14.064
111	3.19	2	288	90.70	1	47.0	9.0	38.0	37.963	20.995
113	6.25	2	289	11.49	1	34.0	9.0	25.0	24.793	**22.096**
114	3.60	1	295	3590.78	6	48.0	34.0	14.0	13.857	19.707
115	6.12	1	296	1427.92	1	48.0	9.0	39.0	38.885	**25.269**
118	1.50	3	297	255.96	1	48.0	9.0	39.0	39.067	**29.270**
122	1.33	4	298	1.00	1	1.0	9.0	-8.0	-7.966	18.472
134	1.42	12	302	13.88	4	35.0	32.0	3.0	2.970	13.976
137	5.75	3	303	138.28	1	48.0	9.0	39.0	38.906	21.206
140	3.47	3	305	8.90	2	32.0	20.0	12.0	11.919	18.513
142	13.31	2	308	1.50	3	7.0	27.0	-20.0	-20.070	7.324
143	26.31	1	312	34.63	4	45.0	32.0	13.0	12.975	8.962
144	18.54	1	313	82.56	1	47.0	9.0	38.0	37.694	17.295
146	66.17	2	314	2.00	1	11.0	9.0	2.0	2.013	12.863
147	9.90	1	315	162.08	1	48.0	9.0	39.0	39.009	20.445
150	4.22	3	319	3.26	4	15.0	32.0	-17.0	-16.991	9.589
157	34.28	7	321	285.91	2	48.0	20.0	28.0	28.120	14.963
161	2.23	4	322	2.00	1	11.0	9.0	2.0	2.165	11.252
162	1.84	1	325	11.57	3	34.0	27.0	7.0	7.075	10.041
163	2.88	1	334	34.70	9	45.0	39.0	6.0	5.823	8.817
164	21.46	1	335	431.00	1	48.0	9.0	39.0	38.985	17.566
165	4.46	1	336	10.89	1	34.0	9.0	25.0	24.916	19.697
166	58.27	1	340	1.00	4	1.0	32.0	-31.0	-30.815	5.049
167	8.84	1	346	1.50	6	7.0	34.0	-27.0	-27.042	0.000
180	1.03	13	347	1.17	1	2.0	9.0	-7.0	-7.185	0.000
187	16.57	7	349	1.27	2	3.0	20.0	-17.0	-16.947	0.000
201	4.96	14	350	26.25	1	42.0	9.0	33.0	32.948	9.555
202	1.37	1	353	11.66	3	34.0	27.0	7.0	6.739	8.738
205	23.39	3	354	3.03	1	13.0	9.0	4.0	3.888	7.332
225	1.70	20	355	12.00	1	34.0	9.0	25.0	25.057	12.472
247	5.30	22	356	1.00	1	1.0	9.0	-8.0	-7.878	6.570
248	15.64	1								
257	5.14	9								

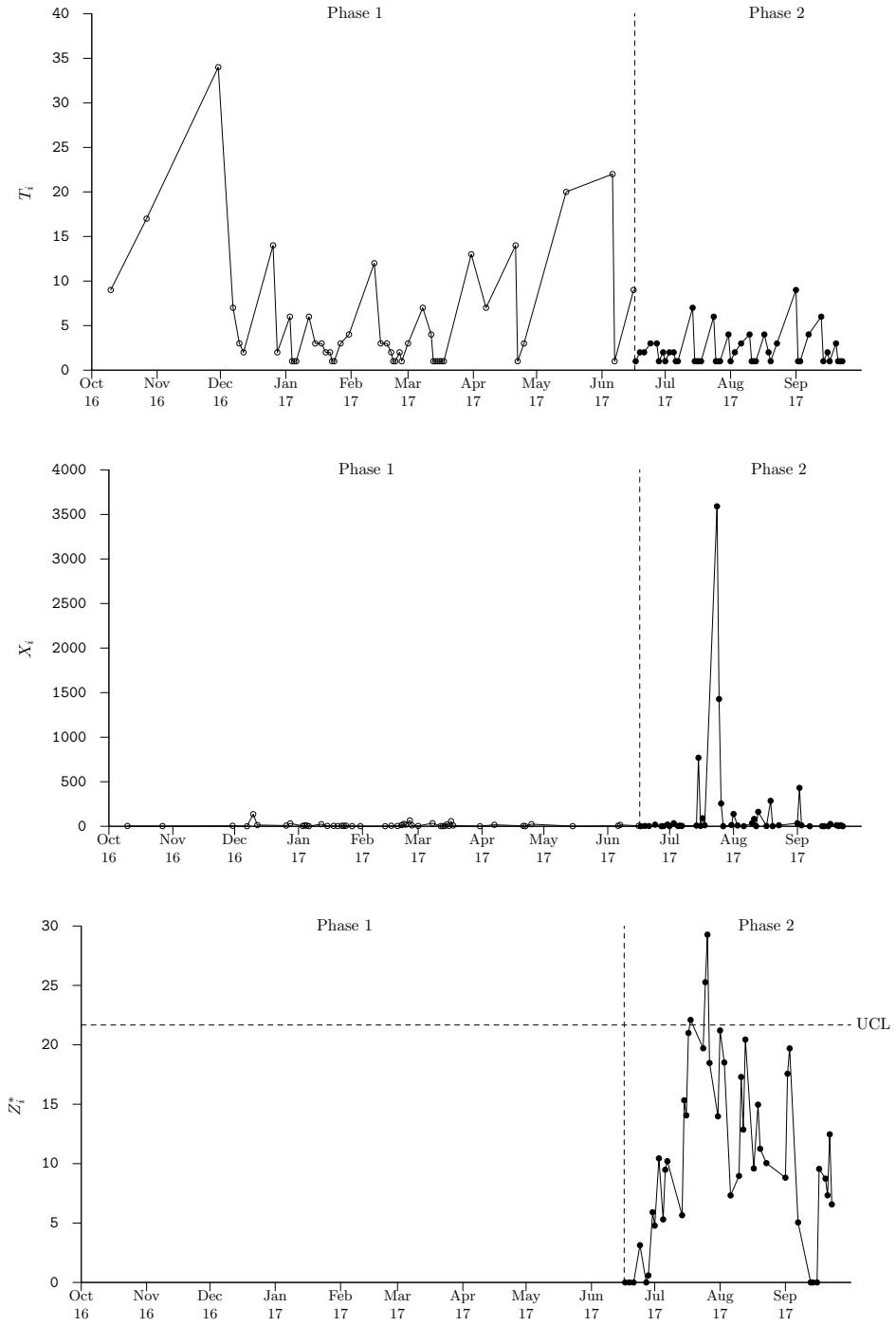

Figure 4: Time T_i in days between fires (top), amplitudes X_i as the burned surface in *ha* (middle) and the rank-based EWMA TBEA chart with statistic Z_i^* (bottom) corresponding to the data set in Table 5

currently available in the literature.

The in-control distribution of the statistics RX and RT used in the rank-based TBEA statistic R is simply a discrete uniform distribution in the set of values $\{1, 2, ..., m+1\}$. Since this distribution does not depend on the parameters of the distributions of X or T, in order to induce out-of-control scenarios, associated with shifts in X and/or T, we used the innovative approach of considering a parameterized distribution that mimics the in- and the out-of-control distributions of the statistics RX and RT. In this paper, we have considered a particular class of beta distributions, that gives equal importance to increases and decreases in the ranks of RX and RT. This choice can have an impact on the type of shift to be detected, and thus, as future research ideas, other parameterizations and classes of distributions can be explored in order to improve the performance of the chart when the shift is mainly due to a change in the amplitude or, on the contrary, to a change in the time between events.

Appendix 1

By definition we have

$$\begin{aligned} \mathrm{V}_0(R_i) = \mathrm{E}_0(R_i^2) &= \sum_{r=-m}^{m} r^2 \frac{m+1-|r|}{(m+1)^2} \\ &= \frac{1}{m+1} \sum_{r=-m}^{m} r^2 - \frac{1}{(m+1)^2} \sum_{r=-m}^{m} r^2|r|. \end{aligned}$$

Using the symmetry allows to sum over $r = 1, \ldots, m$ only

$$\mathrm{V}_0(R_i) = \frac{2}{m+1} \sum_{r=1}^{m} r^2 - \frac{2}{(m+1)^2} \sum_{r=1}^{m} r^3.$$

The first sum reduces to $\frac{1}{6}m(m+1)(2m+1)$ and the second one reduces to $\frac{1}{4}m^2(m+1)^2$ and we have

$$\mathrm{V}_0(R_i) = \frac{m(2m+1)}{3} - \frac{m^2}{2} = \frac{m(m+2)}{6}.$$

Appendix 2

The following self explanatory functions are coded in SciLab (`https://www.scilab.org/`) and they are used in various computations of this paper.

- Compute π_{RT} and π_{RX} in function of p_T and p_X (by solving Equations (12) and (13)). This has been used to populate Table 3.

```
function z=pRp_(pR,p)
  if pR<0.5
    a=pR/(1-pR)
    b=1
  else
```

```
    a=1
    b=(1-pR)/pR
  end
  z=1-p-cdfbeta(0.5,a,b)
endfunction

function pR=pRp(p)
  pR=fsolve1(pRp_,1e-12,1-1e-12,extra=list(p))
endfunction
```

- Compute $f_{\mathrm{RX}}(x)$ (or $f_{\mathrm{RT}}(x)$) in function of m and π_{RX} (or π_{RT}) using Equation (3).

```
function y=pmfRTX(x,m,pR)
  if pR<0.5
    a=pR/(1-pR)
    b=1
  else
    a=1
    b=(1-pR)/pR
  end
  y=zeros(x)
  i=(1<=x)&(x<=m+1)&(floor(x)==x)
  if or(i)
    xi=x(i)
    y(i)=cdfbeta(xi/(m+1),a,b)-cdfbeta((xi-1)/(m+1),a,b)
  end
endfunction
```

- Compute $f_R(x|\pi_{\mathrm{RX}}, \pi_{\mathrm{RT}})$ based on Equation (5).

```
function y=pmfR(x,m,pRX,pRT)
  y=zeros(x)
  for i=1:m+1
    y=y+pmfRTX(x+i,m,pRX)*pmfRTX(i,m,pRT)
  end
endfunction
```

- Compute $F_{R^*}(x|\pi_{\mathrm{RX}}, \pi_{\mathrm{RT}})$ using Equation (6).

```
function y=cdfRs(x,m,pRX,pRT,sd)
  y=zeros(x)
  for i=-m:m
    y=y+pmfR(i,m,pRX,pRT)*cdfnormal(x,i,sd)
  end
endfunction
```

- Compute $f_{R^*}(x|\pi_{\mathrm{RX}}, \pi_{\mathrm{RT}})$ using Equation (7).

```
function y=pdfRs(x,m,pRX,pRT,sd)
```

```
  y=zeros(x)
  for i=-m:m
    y=y+pmfR(i,m,pRX,pRT)*pdfnormal(x,i,sd)
  end
endfunction
```

- Computation of the ARL and SDRL of the rank-based EWMA TBEA chart based on formulas presented within Equations (9) and (11).

```
function [ARL,SDRL]=rlRBEWMATBEA(K,lam,m,pRX,pRT)
  [lhs,rhs]=argn()
  sd=0.125
  s=100
  s1=s+1
  UCL=K*sqrt(lam/(2-lam)*(sd*sd+m*(m+2)/6))
  Delta=UCL/(2*s)
  h=[0,linspace(Delta,UCL-Delta,s)]'
  Hi=h*ones(1,s1)
  Hj=Hi'
  Q1=(Hj+Delta-(1-lam)*Hi)/lam
  Q2=(Hj-Delta-(1-lam)*Hi)/lam
  Q=cdfRs(Q1,m,pRX,pRT,sd)-cdfRs(Q2,m,pRX,pRT,sd)
  Q(:,1)=cdfRs(-(1-lam)*h/lam,m,pRX,pRT,sd)
  q=[1;zeros(s,1)]
  W=inv(eye(s1,s1)-Q)
  Z=q'*W
  ARL=sum(Z)
  if lhs==2
    Z=Z*W*Q
    SDRL=sqrt(2*sum(Z)+ARL*(1-ARL))
  end
endfunction
```

Acknowledgements

This work is partially financed by national funds through FCT – Fundação para a Ciência e a Tecnologia under the project UIDB/00006/2020. DOI: 10.54499/UIDB/00006/2020 (https://doi.org/10.54499/UIDB/00006/2020).

Disclosure Statement

No potential competing interest was reported by the author(s).

References

H. Ahmad, A. Ahmadi Nadi, M. Amini, and B. Sadeghpour Gildeh. Monitoring Processes with Multiple Dependent Production Lines using Time Between Events Control Charts. *Quality Engineering*, 35(4):639–668, 2023.

S. Ali. A Predictive Bayesian Approach to Sequential Time-Between-Events Monitoring. *Quality and Reliability Engineering International*, 36(1):365–387, 2020.

S. Ali. First Passage Time Control Charts assuming Power Law Intensity for Time to Jointly Monitor Time and Magnitude. *Quality and Reliability Engineering International*, 37(5):2034–2064, 2021.

S. Ali and A. Pievatolo. Time and Magnitude Monitoring based on the Renewal Reward Process. *Reliability Engineering & System Safety*, 179:97–107, 2018.

K. Anojahatlo and K. Sabri-Laghaie. Enhancing the Detection Power of Multivariate Time Between Events Control Charts for Gumbel's Bivariate Exponential Distribution. *Computers & Industrial Engineering*, 171:108215, 2022.

D. Brook and D.A. Evans. An approach to the probability distribution of CUSUM run length. *Biometrika*, 59(3):539–549, 1972.

P. Castagliola, K.P. Tran, G. Celano, A.C. Rakitzis, and P.E. Maravelakis. An EWMA-type Sign Chart with Exact Run Length Properties. *Journal of Quality Technology*, 51(1):51–63, 2019. doi: 10.1080/00224065.2018.1545497.

G. Celano, P. Castagliola, S. Chakraborti, and G. Nenes. On the Implementation of the Shewhart Sign Control Chart for Low-Volume Production. *International Journal of Production Research*, 54(19):5886–5900, 2016. doi: 10.1080/00207543.2016.1186297.

S. Chakraborti and M.A. Graham. Nonparametric (Distribution-Free) Control Charts: An Updated Overview and Some Results. *Quality Engineering*, 31 (4):523–544, 2019a.

S. Chakraborti and M.A. Graham. *Nonparametric Statistical Process Control*. John Wiley & Sons, 2019b.

S. Chakraborti, P. van der Laan, and S.T. Bakir. Nonparametric Control Charts: an Overview and Some Results. *Journal of Quality Technology*, 33(3):304–315, 2001.

S. Chakraborti, N. Kumar, A.C. Rakitzis, and R.S. Sparks. Time Between Events Monitoring with Control Charts. *Wiley StatsRef: Statistics Reference Online*, pages 1–13, 2014. doi: 10.1002/9781118445112.stat08409.

Y. Cheng and A. Mukherjee. One Hotelling t^2 Chart based on Transformed Data for Simultaneous Monitoring the Frequency and Magnitude of an Event. In *2014 IEEE International Conference on Industrial Engineering and Engineering Management*, pages 764–768, 2014. doi: 10.1109/IEEM.2014.7058741.

Y. Cheng, A. Mukherjee, and M. Xie. Simultaneously Monitoring Frequency and Magnitude of Events based on Bivariate Gamma Distribution. *Journal of Statistical Computation and Simulation*, 87(9):1723–1741, 2017.

E. Dogu and M. Noor ul Amin. Monitoring Exponentially Distributed Time Between Events Data: Self-Starting Perspective. *Communications in Statistics-Simulation and Computation*, 52(3):1104–1118, 2023.

X.L. Hu, Y.L. Qiao, P.P. Zhou, J.L. Zhong, and S. Wu. Modified One-Sided EWMA Charts for Monitoring Time Between Events. *Communications in Statistics-Simulation and Computation*, 52(3):1041–1056, 2023.

A. Johannssen, N. Chukhrova, G. Celano, and P. Castagliola. A Number-Between-Events Control Chart for Monitoring Finite Horizon Production Processes. *Quality and Reliability Engineering International*, 38(4):2110–2138, 2022. doi: 10.1002/qre.3068.

N. Kumar and S. Chakraborti. Phase II Shewhart-Type Control Charts for Monitoring Times Between Events and Effects of Parameter Estimation. *Quality and Reliability Engineering International*, 32(1):315–328, 2016.

G. Ozsan, M.C. Testik, and C.H. Weiß. Properties of the Exponential EWMA Chart with Parameter Estimation. *Quality and Reliability Engineering International*, 26(6):555–569, 2010.

C. Pehlivan and M.C. Testik. Impact of Model Misspecification on the Exponential EWMA Charts: a Robustness Study when the Time-Between-Events are not Exponential. *Quality and Reliability Engineering International*, 26 (2):177–190, 2010.

T. Perdikis, S. Psarakis, P. Castagliola, and G. Celano. An EWMA-type Chart based on Signed Ranks with Exact Run Length Properties. *Journal of Statistical Computation and Simulation*, 91(4):732–751, 2021a. doi: 10.1080/00949655.2020.1828415.

T. Perdikis, S. Psarakis, P. Castagliola, and P.E. Maravelakis. An EWMA Signed Ranks Control Chart with Reliable Run Length Performances. *Quality and Reliability Engineering International*, 37(3):1266–1284, 2021b. doi: 10.1002/qre.2795.

L. Qu, Z. Wu, M.B.C. Khoo, and P. Castagliola. A CUSUM Scheme for Event Monitoring. *International Journal of Production Economics*, 145(1):268–280, 2013. doi: 10.1016/j.ijpe.2013.04.048.

L. Qu, S. He, M.B.C. Khoo, and P. Castagliola. A CUSUM Chart for Detecting the Intensity Ratio of Negative Events. *International Journal of Production Research*, 56(19):6553–6567, 2018. doi: 10.1080/00207543.2017.1398423.

D. Rahali, P. Castagliola, H. Taleb, and M.B.C. Khoo. Evaluation of Shewhart Time-Between-Events-and-Amplitude Control Charts for Several Distributions. *Quality Engineering*, 31(2):240–254, 2019. doi: 10.1080/08982112.2018.1479036.

D. Rahali, P. Castagliola, H. Taleb, and M.B.C. Khoo. Evaluation of Shewhart Time-Between-Events-and-Amplitude Control Charts for Correlated Data. *Quality and Reliability Engineering International*, 37(1):219–241, 2021. doi: 10.1002/qre.2731.

C. Rizzo, S.T. Chin, E. van den Heuvel, and A. Di Bucchianico. Performance Measures of Discrete and Continuous Time-Between-Events Control Charts. *Quality and Reliability Engineering International*, 36(8):2754–2768, 2020.

D. Roy and T. Dasgupta. A Discretizing Approach for Evaluating Reliability of Complex Systems under Stress-Strength Model. *IEEE Transactions on Reliability*, 50(2):145–150, 2001.

R.A. Sanusi, S.Y. Teh, and M.B.C Khoo. Simultaneous Monitoring of Magnitude and Time-Between-Events Data with a Max-EWMA Control Chart. *Computers & Industrial Engineering*, 142:106378, 2020.

A.A Tang, J. Sun, X.L. Hu, and P. Castagliola. A New Nonparametric Adaptive EWMA Control Chart with Exact Run Length Properties. *Computers & Industrial Engineering*, 130:404–419, 2019. doi: 10.1016/j.cie.2019.02.045.

S. Wu, P. Castagliola, and G. Celano. A Distribution-Free EWMA Control Chart for Monitoring Time-Between-Events-and-Amplitude Data. *Journal of Applied Statistics*, 48(3):434–454, 2021. doi: 10.1080/02664763.2020.1729347.

S. Wu, P. Castagliola, A.C. Rakitzis, and P.E. Maravelakis. Design of Attribute EWMA Type Control Charts with Reliable Run Length Performance. *Communications in Statistics – Simulation and Computation*, 52(9):4193–4209, 2023.

Z. Wu and L. Qu. A Single Chart for Monitoring Frequency and Magnitude of Events. In *2010 IEEE International Conference on Industrial Engineering and Engineering Management*, pages 1416–1420, 2010. doi: 10.1109/IEEM.2010.5674350.

Z. Wu, J. Jiao, and Z. He. A Control Scheme for Monitoring the Frequency and Magnitude of an Event. *International Journal of Production Research*, 47(11):2887–2902, 2009a.

Z. Wu, J. Jiao, and Z. He. A Single Control Chart for Monitoring the Frequency and Magnitude of an Event. *International Journal of Production Economics*, 119(1):24–33, 2009b.

F.P. Xie, P. Castagliola, Y.L. Qiao, X.L. Hu, and J.S. Sun. A One-Sided Exponentially Weighted Moving Average Control Chart for Time Between Events. *Journal of Applied Statistics*, 49(15):3928–3957, 2022a. doi: 10.1080/02664763.2021.1967894.

F.P. Xie, P. Castagliola, J.S. Sun, A.A. Tang, and X.L. Hu. A One-Sided Adaptive Truncated Exponentially Weighted Moving Average Scheme for Time Between Events. *Computers & Industrial Engineering*, 168:108052, 2022b. doi: 10.1016/j.cie.2022.108052.

Y. Xie, M. Xie, and T.N. Goh. Two MEWMA Charts for Gumbel's Bivariate Exponential Distribution. *Journal of Quality Technology*, 43(1):50–65, 2011.

S.F. Yang and S.W. Cheng. A New Non-Parametric CUSUM Mean Chart. *Quality and Reliability Engineering International*, 27(7):867–875, 2011.

S.F. Yang, J.S. Lin, and S.W. Cheng. A New Nonparametric EWMA Sign Control Chart. *Expert Systems with Applications*, 38(5):6239–6243, 2011.

M. Zhang, F.M. Megahed, and W.H. Woodall. Exponential CUSUM Charts with Estimated Control Limits. *Quality and Reliability Engineering International*, 30(2):275–286, 2014.

I.M. Zwetsloot, T. Mahmood, and W.H. Woodall. Multivariate Time-Between-Events Monitoring: An Overview and Some Overlooked Underlying Complexities. *Quality Engineering*, 33(1):13–25, 2021.